CoMFA 3D-QSAR Analysis of HIV-1 RT Non-nucleoside inhibitors, TIBO Derivatives based on Docking conformation and alignment

Zhigang Zhou, Jeffry D. Madura*

Department of Chemistry and Biochemistry, Duquesne University, Pittsburgh, PA 15282.

* To whom correspondence should be addressed,

e-mail: madura@duq.edu

Phone: 412-396-6341

Fax: 412-396-5683

3D-QSAR Analysis of HIV-1 RT Non-nucleoside inhibitors, TIBO Derivatives based on CoMFA, CoMSIA, and Docking

Zhigang Zhou, Jeffry D. Madura

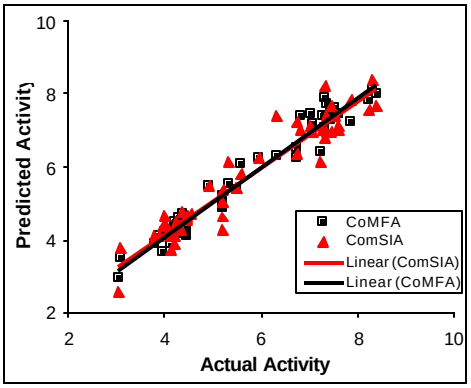

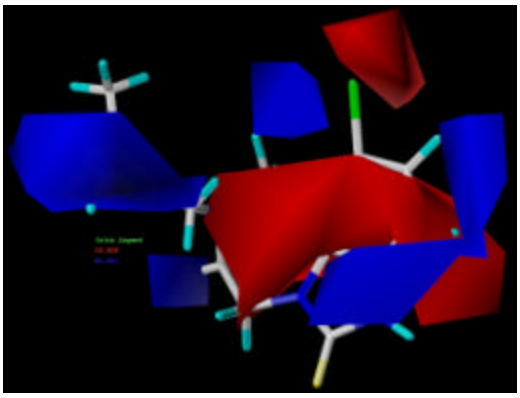

Abstract:

HIV-1 RT is one of the key enzymes in the duplication of HIV-1. Inhibitors of HIV-1 RT are classified as non-nucleoside RT inhibitors (NNRTIs) and nucleoside analogues. NNRTIs bind in a region not associated with the active site of the enzyme. Within the NNRTI category, there is a set of inhibitors commonly referred to as TIBO inhibitors. 52 TIBO inhibitors were used in the work to build 3-D QSAR models. The alignment of molecules and "active" conformation selection are key to a successful 3D-QSAR model by CoMFA. The flexible docking (Autodock3) was used on determination of "active" conformation and molecular alignment and CoMFA and CoMSIA were used to develop 3D-QSAR models of 52 TIBOs in the work. The 3D QSAR models demonstrate good ability to predict activity of studied compounds (r^2 = 0.962, 0.948, q^2 = 0.701, 0.708). It is shown that the steric and electrostatic properties predicted by CoMFA contours can be related to the binding structure of the complex. The results demonstrate that combination of ligand-based and receptor-based modeling is a powerful approach to build 3D-QSAR models.

Keywords

HIV-1 RT, TIBO, 3D QSAR, Docking, PLS, CoMFA, CoMSIA.

Introduction

The Reverse Transcriptase of Human Immunodeficiency Virus type 1 (HIV-1 RT) function is to transcribe a single-stranded viral RNA genome into double-stranded DNA and plays a vital role in the replication of HIV-1.[1-4] Several drugs that target this enzyme have been approved to treat Acquired Immune Deficiency Syndrome (AIDS). There are two types of RT inhibitors. One type of RT inhibitor is commonly referred to as a nucleoside inhibitor. This inhibitor inserts as nucleoside analogue into DNA and acts as chain-terminating agent, therefore, terminating viral synthesis. The other type is called the non-nucleoside inhibitor (NNRTI).[5-12] NNRTIs bind in a non-nucleoside binding pocket (NNBP) to inhibit the activity of RT. TIBO and its derivatives are a class of NNRTIs that have demonstrated good activity towards RT inhibition. One (Tivirapine) of them has moved onto the clinical development cycle.[8] The crystal structures of several TIBOs/RT complexes are currently available.[13,14] These complexes provide some insight into the binding and interactions of TIBOs in RT. However the inhibition model of TIBOs still needs to be elucidated in order to find and design new and more potent inhibitors that remain effective to HIV-1 RT mutants due to the presence of NNRTIs.

Docking is one method in which the binding of an inhibitor to a receptor can be explored.[15-23] Comparative molecular field analysis (CoMFA)[24] and comparative molecular similarity indices analysis (CoMSIA)[25,26] are powerful and versatile tools to build and design an activity model (QSAR) for a given set of molecules in rational drug design and related applications.[27-36] Recently, we use an Autodock3 to successfully dock a set of NNRTIs into RT. The calculated binding energies, based on the docked

structures, agree well with the experimental activities.[37] QSAR models of 46 TIBOs were studied by Hannongbua et al.[38] using CoMFA and by Huuskonen[39] based on the atom level E-state indices and calculated molecular properties (*logP, MR*). Also the correlation between activities and logP of several sets of TIBOs were explored by Garg et al.[40] Some works show that the binding affinity calculated by Monte Carlo and Linear Response equation has good correlation with the activity of TIBOs.[41,42]

In CoMFA or other 3D-QSAR studies, the molecule alignment and conformation determination are so important that they affect the success of a model. In most cases a bound TIBO/RT complex is not available and therefore a computation method has to be deployed to determine conformations and alignment of a set of molecules so that 3-D QSAR work can be carried out. Several strategies have been used to determine conformation and align molecules. Of them, docking is an attractive way to align molecules for CoMFA. Several applications of docking alignment with CoMFA have been reported.[43-45]

In this paper, determination of the "active" conformation of each molecule and the molecular alignment are done using the flexible docking program, Autodock3.[46] The molecular alignment is done according to the electrostatic and structural properties of the active site of RT. Then 3D-QSAR models based on the active conformation and the aligned cluster are constructed using CoMFA and CoMSIA. The strategy of combining conformations and alignment obtained from the Autodock3 with the CoMFA produces a natural and reasonable elucidation of activation from a 3D-QSAR calculation.

Methods

Data Set and Molecule Preparation.

The construction and preparation of molecular coordinates of all molecules were done using Molecular Operating Environment (MOE) program (Chemical Computing Group, Montreal, Canada). The starting coordinates of the HIV-1 RT/TIBO complex (1REV) were taken from the Protein Data Bank[14]. After hydrogen atoms were added using MOE, the substrate (9Cl-TIBO) and the protein (RT) were saved separately. Partial charges for the protein were assigned from the AMBER94 force field.[47] The protein was minimized holding all non-hydrogen atoms fixed. All other inhibitors were built using the 9Cl-TIBO as a template. The PEOE charge set[48] was used on the ligands and full optimization was performed to minimize each structure. The structure and experimental activity (pIC_{50}) for the inhibitors used in this work are list in **Table 1**.[49-53]

Docking Simulation.

Autodock3[46] was used in this study to perform the docking simulations. All single bonds of a substrate were allowed to rotate freely. The Lammarckian Genetic Algorithm (LGA)[54] in Autodock3 was used to explore the energy landscape. The hybrid search technique consists of a global optimizer[55] modified from a genetic algorithm with 2-point crossover, random mutation, and a local optimizer with a Solis and Wets algorithm. A docking box of 60x60x60 points with a grid spacing of 0.375 Å was used in the

calculations. Random conditions were used in the settings of seed, initial quaternion, coordinates and torsions. A 0.2 Å step was used for translation and a 25-degree was used for quaternion and torsion. The maximum number of energy evaluation was 250,000 and the maximum number of generations was 27,000. The rate of gene mutation was 0.02 and the rate of crossover was 0.8. The number of cycles was set to 20. So a total of 20 docking configurations were determined in each docking calculation. The "preferable" docking configuration, which was chosen based on the lowest empirical binding free energy and the most frequent cluster[37], was chosen as the "active" binding conformation. This conformation was used in two alignment schemes as "bioactive" confromation.

Alignment.

The program SYBYL (version 6.8) was used in the development of the 3D-QSAR models. CoMFA and CoMSIA studies require the coordinates of molecules to be aligned according to reasonable bioactive conformations. In this case we used the conformation obtained from our docking calculations as the "bioactive" conformation needed in the alignment step. Two alignment schemes were used to build the 3D-QSAR models. Scheme 1 is that the relative binding positions of all molecules obtained from the docking calculations were used. In other words, the alignment was done using flexible docking based on the steric and electrostatic properties of the binding pocket of the receptor (RT). Scheme 2 is to use the *Atom Fit* method in SYBYL. The 9Cl-TIBO was used as a template to align the remaining inhibitor molecules. The core structure used for the

alignment is shown in **Figure 1**. The reference atoms, marked black in the figure, are all in one plane and were used to align all other molecules.

CoMFA and CoMSIA 3D QSAR Models.

CoMFA[24] and CoMSIA[25,26] descriptors were calculated using the following parameters. A 3D grid spacing of 2 Å in x, y and z directions and an extension of 4 Å beyond the aligned molecules in all directions are used. An sp^3 carbon probe atom with a charge of +1.0 and a vdW radius of 1.52 Å was used to calculated CoMFA steric and electrostatic field descriptors. The distant-depended dielectric constant was used for treating electrostatic term. A default cutoff of 30 kcal/mol was used to truncate the steric field and electrostatic field energies. The CoMFA standard method was used for scaling.

CoMSIA[25,26] calculates the similarity descriptors by way of a grid lattice. For a molecule j with atoms i at the grid point q, the CoMSIA similarity indices A_F are calculated by the equation as follows:

$$A_{F,k}^{q}(j) = -\sum \omega_{probe,k}\omega_{jk}e^{-ar_{iq}^2}$$

Where ω_{jk} is the actual value of the physicochemical property k of atom i; $\omega_{probe,k}$ is the property of probe atom with pre-set charge (+1 in this case), radius (1.53 Å), and hydrophobicity of 1; and r_{iq} is the mutual distance between the probe atom at grid point q and atom i of the molecule. In the CoMSIA calculations, five physicochemical properties (steric, electrostatic, hydrophobic, hydrogen bond donor, and hydrogen bond acceptor) were determined for all of the molecules. The same parameters used in the CoMFA calculations were used here.

PLS Analysis.

After all of the CoMFA and CoMSIA descriptors were calculated, Partial Least-Squares analysis (PLA) was performed to obtain a 3D QSAR model. The PLS method has been used in numerous applications in correlating the activity with various physicochemical properties. The PLS regression tries to build a relationship between a dependent variable (normally a activity) and several independent variables (property descriptors). The CoMFA standard scaling and column filtering of 2.0 were used in PLS analysis.

Cross-validations in PLS were done by the leave-one-out procedure to find out the optimal number of components in building the regression models and to check statistic significance of models. The leave-one-out technique provides a good way to quantitatively evaluate the internal predictive ability of a model by removing a one compound out at a time and then building the QSAR model and calculating the activity of the compound using the newly model constructed from the remaining compounds in the data set. The quality of a model is expressed as the cross-validated correlation coefficient q^2.

The optimal number of components is the smallest cross-validated standard error of estimate SE_{press} (or the number giving the largest value of q^2, as they are consistent in most time).

The optimal number of components obtained is then used to derive the final QSAR model using all the compounds (without cross-validation). The conventional correlation coefficient (r^2) is used to measure the quality of the model.

Results and Discussions

Docking and Atom Fit Alignments.

As previously stated, the conformation of each compound was obtained from docking calculations. Two alignments (Atom fit and flexible docking) were used to explore the effect of molecular alignment on the CoMFA and CoMSIA analysis. The aligned molecules by docking and atom fit are shown in **Figure 2** and **Figure 3**, respectively. In **Figure 3**, one observes that the overall overlap is clear. Compared with **Figure 2**, it can be seen that the cluster of molecules aligned by the atom fit method is better than the cluster aligned by docking in term three rings overlap. The biggest different is with the substrate groups (especially the R group). On the other hand, the docking alignment produced different clusters of molecules as it aligns each molecule at its preferable binding position in the active site of RT. From the **Figure 2**, it can be seen that the positions of rings are different for each molecule.

QSAR Models.

The statistical results of CoMFA and CoMSIA studied are summarized in **Table 2**. These analyses were based on the clusters of molecules that were aligned by the two methods. The regression coefficient (r^2) and the cross-validation coefficient (q^2) of the QSAR model constructed by CoMFA based on the docking alignment are 0.962 and 0.701, respectively. The two coefficients for the CoMSIA model are 0.948 and 0.708,

respectively. Based on the coefficient values, the CoMFA and CoMSIA yielded similar QSAR models (CoMFA model appears slightly better than CoMSIA). Both models exhibit good predictive capabilities as shown by the leave-one-out method. The standard errors of estimate for the two models are 0.326 and 0.381, respectively.

In the QSAR models based on the atom fit alignment, the regression coefficient (r^2) and the cross-validation coefficient (q^2) for CoMFA models are 0.959 and 0.661, respectively. The two coefficients of CoMSIA model are 0.916 and 0.680, respectively. The coefficients are all slight smaller than the corresponding values of docking alignment models. Although the differences are not large, they show that the docking alignment models are slightly better than atom fit alignment models.

The CoMFA and CoMSIA calculated electrostatic and steric properties (descriptors) are based on the grid built around these molecules. In the atom fit system, the largest difference between these calculated properties for these molecules derives from the side chain groups rather than the three rings (A, B and C). On the other hand, in the docking alignment system, the difference between these calculated properties derives from all the atoms.

Also it is observed that with the CoMFA results, the steric and electrostatic contributions are not very difference (0.41 vs. 0.59 in docking alignment, 0.50 vs. 0.50 in atom fit alignment). The electrostatic contributions in the CoMSIA models are nearly three fold of the steric contributions. It is also observed that the hydrophobic contributions are the largest part in CoMSIA models. This is consistent with the concept that the NNRTI active site of RT is hydrophobic. In our docking[37] works, it was recognized that the hydrophobic part of a NNRTI binds inside and a water bridge

network forms between hydrophilic atoms of NNRTI and residues around the entrance of the active site. It is believed that this water network helps stabilize the binding of NNRTI in RT. These results support the idea that the hydrophobic and hydrophilic properties of NNRTIs are important in the design of NNRTIs.

The calculated activity vs. experimental activity of each compound using the atom fit and docking models is shown in **Figure 4**. The black squares and red triangles are CoMFA and CoMSIA results based on docking alignment and conformation determination. The green diamonds and yellow cycles are CoMFA and CoMSIA results based on atom fit alignment and docking conformation determination. The black line is the trend line of the CoMFA model of docking and the green line is the trend line of the CoMFA model of atom fit. It is seen that the trend lines of CoMFA models based on the docking and atom fit are nearly identical. The fits are nearly perfect with a slop of near 1. It indicats that the CoMFA and CoMSIA models do not have a systematic deviation.. The prediction residuals for both models are shown in **Figure 5**. It is observed that the CoMFA model (black and green) has fewer long-bars than the CoMSIA model (red and yellow). This means that the CoMFA model yields a little better prediction than the CoMSIA model. In **Table 2**, it is seen that the CoMFA models have r^2 values of 0.962 and 0.959 for docking model and atom fit model, respectively, which are slightly higher than CoMSIA models' r^2 values of 0.948 and 0.916, respectively. On the other hand, the q^2 value of the CoMFA models is slightly smaller than that of the CoMSIA models.

Graphical Interpretation of the Results.

To further explore the hypothetical interaction of a ligand with its receptor, the steric and electrostatic contour maps of the CoMFA model from docking model are shown in **Figure 6** and **Figure 7**. The compound 8-Cl-TIBO (Tivirapine, pIC_{50} =8.37) is used in the figures for analysis. Considering the steric contour first, it is seen that there are two regions where the addition of bulky groups may increase activity. One is in the direction of the R group. It indicates that changing to a larger linear group from the methyl group will increase the activity of the ligand. The other region is near the 8 position of ring A above the ring plane. A non-favorable region is indicated at the region below the ring plane in the same direction. There are several regions in yellow around the R position which indicates that smaller groups may increase activity. Checking the bound complex of this compound and RT (modeled from crystal structure of RT complex) shown in **Figure 8**, it is seen that there is extra room near the region of the methyl group which corresponds to the green region in the CoMFA steric contour. In addition there is no extra room in the region of the methyl group which corresponds to the yellow region on the CoMFA steric map. It is also seen that Tivirapine in the complex makes good contact with the protein near the linking area of the R group of ring B. The predicted results from the steric CoMFA contour are consistent with the calculated complex.

The electrostatic contour map (**Figure 7**), the positive-favorable regions (blue) are roughly around the entire molecule except the area near the 8 and 9 positions of ring A (indicated in red). Compared with bound complex (**Figure 8**), the positive area at the R position of the molecule matches the negative (red) area of the active site of RT. The region of the active site where the 1 and 10 positions of rings bind is also negative (red) area. The area on the ligand matches the positive-favorable areas (blue). Based on the steric and electrostatic properties comparison between the CoMFA contours and bound complex, it is seen that the predictions by the contours can be related to binding characteristics.

Conclusions

The satisfactory 3D-QSAR models of 52 TIBO derivatives have been constructed using CoMFA and CoMSIA methods based on the docking conformation determination and two molecular alignments. They demonstrate that flexible docking is a good method to determinate the "active" conformation of molecules for 3D-QSAR analyses. The combination of flexible docking with CoMFA is an attractive way to construct 3D-QSAR models.

The CoMFA QSAR models show that the steric part and electrostatic part contribute equally to the activity. The CoMSIA QSAR models show that the largest contribution comes from the hydrophobic part. This was supported by our previous docking results that hydrophobic and hydrophilic interactions are important for NNRTI binding in RT active site.

The steric and electrostatic contours from CoMFA provide some useful insight into designing novel inhibitors with increased activity. By comparing these predictions from the CoMFA contours and the bound complex of RT/8-Cl-TIBO, we can see that part of the prediction is consistent with the characteristics of the inhibitor and RT.

A ligand-based approach is used in rational drug design to build activity models, which provide important information on possible improvements in ligand structure to increase activity. Meanwhile receptor-based modeling provides an insight into the interaction model of a ligand in its receptor and aids in new ligand design. Both approaches provide a powerful approach in building 3D-QSAR models.

Acknowledgements

The authors would like to thank Dr. Aleem Gangjee for allowing to access the computational resources in his group and Mr. Xing Lin for his help. This research was supported in part by a grant from the National Computational Science Alliance (MCB990008Nr00).

References

(1) Jacobo-Molina, A.; Arnold, E. HIV reverse transcriptase structure-function relationships. *Biochemistry* **1991**, *30*, 6351-6361.

(2) Le Grice, S. F. J. Human immunodeficiency virus reversee transcriptase. *Reverse transcriptase*; Cold spring Harbor Laboratory Press: Plainview, NY, 1993; pp 163-191.

(3) Goff, P. Retroviral reverse transcriptase: Synthesis, structure and function. *J. Acquired Immune Definciency Syndromes* **1990**, *3*, 817-831.

(4) Whitcomb, J. M.; Hughes, S. H. Retroviral reverse transcription and integration: Progress and problems. *Annu. Rev. Cell Biol.* **1992**, *8*, 275-306.

(5) Arnold, E.; Das, K.; Ding, J.; Yadav, P.; Hsiou, Y. et al. Targeting HIV reverse transcriptase for anti-AIDS drug design: structural and biological considerations for chemotherapeutic strategies. *Drug Design Discov.* **1996**, *13*, 29-47.

(6) Larder, B. A. Inhibitors of HIV reverse transcriptase as antiviral agents and drug resistence. *Reverse Transcriptase*; Cold spring Harbor Laboratory Press: Plainview, NY, 1993; pp 163-191.

(7) Tantillo, C.; Ding, J.; Jacobo-Molina, A.; Nanni, R. G.; Boyer, P. L. et al. Locations of anti-AIDS drug binding sites and resistance mutations in the three-dimensional structure of HIV-1 reverse transcriptase: implications for mechanisms of drug inhibition and resistance. *J. Mol. Biol.* **1994**, *243*, 369-387.

(8) De Clercq, E. Antiviral therapy for human immunodeficiency virus infections. *Cln. Microbiol. Rev.* **1995**, *8*, 200-239.

(9) Ding, J.; Das, K.; Hsiou, Y.; Zhang, W.; Arnold, E. et al. Structural Studies of HIV-1 Reverse Transcriptase and Implications for Drug Design. *Structure-Based Drug Design* **1997**, 41-82.

(10) Pedersen, O. S.; Pedersen, E. B. non-nuleosid reverse transcriptase inhibitors. *Antiviral Chem. Chemother.* **1999**, *10*, 285-314.

(11) Koup, R. A.; Merluzzi, V. J.; Hargrave, k. D.; Adems, J.; Grozinger, K. et al. Inhibition of human immunodeficiency virus type1 replication by the dipyridocliazepinone BI-RG-587. *J. infect. Dis.* **1991**, *163*, 966-970.

(12) Richman, D.; Rosenthal, A. S.; Shoog, M.; Eckner, R. J.; Chou, T. C. et al. BI-RG-587 in active against zidovudine-pesisant human immunodedeficiency virus type 1 and synegistic with zidovudine. *Antimicrob. Agents chemother.* **1991**, *35*, 305-308.

(13) Das, K.; Ding, J.; Hsiou, Y.; Clark, A. J.; Moereels, H. et al. Crystal structures of 8-Cl and 9-Cl TIBO complexed with wild-type HIV-1 RT and 8-Cl TIBO complexed with the Tyr181Cys HIV-1 RT drug-resistant mutant. *J Mol. Biol.* **1996**, *264*, 1085-1100.

(14) Ren, J.; Esnouf, R.; Hopkins, A.; Ross, C.; Jones, Y. et al. The structure of HIV-1 reverse transcriptase complexed with 9-chloro-TIBO: lessons for inhibitor design. *Structure* **1995**, *3*, 915-926.

(15) Dominguez, C.; Boelens, R.; Bonvin, A. M. J. J. HADDOCK: A Protein-Protein Docking Approach Based on Biochemical or Biophysical Information. *Journal of the American Chemical Society* **2003**, *125*, 1731-1737.

(16) Jain, A. N. Surflex: Fully Automatic Flexible Molecular Docking Using a Molecular Similarity-Based Search Engine. *Journal of Medicinal Chemistry* **2003**, *46*, 499-511.

(17) Johnson, M. A.; Hoeoeg, C.; Pinto, B. M. A Novel Modeling Protocol for Protein Receptors Guided by Bound-Ligand Conformation. *Biochemistry* **2003**, *42*, 1842-1853.

(18) Zhou, Z.; Fisher, D.; Spidel, J.; Greenfield, J.; Patson, B. et al. Kinetic and Docking Studies of the Interaction of Quinones with the Quinone Reductase Active Site. *Biochemistry* **2003**, *42*, 1985-1994.

(19) Wu, X.; Milne, J. L. S.; Borgnia, M. J.; Rostapshov, A. V.; Subramaniam, S. et al. A core-weighted fitting method for docking atomic structures into low-resolution maps: Application to cryo-electron microscopy. *Journal of Structural Biology* **2003**, *141*, 63-76.

(20) Todorov, N. P.; Mancera, R. L.; Monthoux, P. H. A new quantum stochastic tunnelling optimisation method for protein-ligand docking. *Chemical Physics Letters* **2003**, *369*, 257-263.

(21) Wang, L.; Merz, A. J.; Collins, K. M.; Wickner, W. Hierarchy of protein assembly at the vertex ring domain for yeast vacuole docking and fusion. *Journal of Cell Biology* **2003**, *160*, 365-374.

(22) Vicker, N.; Ho, Y.; Robinson, J.; Woo, L. L. W.; Purohit, A. et al. Docking studies of sulphamate inhibitors of estrone sulphatase in human carbonic anhydrase II. *Bioorganic & Medicinal Chemistry Letters* **2003**, *13*, 863-865.

(23) Sabnis, Y. A.; Desai, P. V.; Rosenthal, P. J.; Avery, M. A. Probing the structure of falcipain-3, a cysteine protease from plasmodium falciparum: Comparative protein modeling and docking studies. *Protein Science* **2003**, *12*, 501-509.

(24) Cramer, R. D. I.; Patterson, D. E.; Bunce, J. D. Comparative molecular field analysis (CoMFA). 1. Effect of shape on binding of steroids to carrier proteins. *J. Am. Chem. Soc.* **1988**, *110*, 5959-5967.

(25) Klebe, G.; Abraham, U.; Mietzner, T. Molecular Similarity Indices in a Comparative Analysis (CoMSIA) of Drug Molecules to Correlate and Predict Their Biological Activity. *J. Med. Chem.* **1994**, *37*, 4130-4146.

(26) TBohm, M.; Sturzebecher, J.; Klebe, G. hree-Dimensional Quantitative Structure-Activity Relationship Analyses Using Comparative Molecular Field Analysis and Comparative Molecular Similarity Indices Analysis To Elucidate Selectivity Differences of Inhibitors Binding to Trypsin, Thrombin, and Factor Xa. *J. Med. Chem.* **1999**, *42*, 458-477.

(27) Buolamwini, J. K.; Assefa, H. CoMFA and CoMSIA 3D QSAR and Docking Studies on Conformationally-Restrained Cinnamoyl HIV-1 Integrase Inhibitors: Exploration of a Binding Mode at the Active Site. *Journal of Medicinal Chemistry* **2002**, *45*, 841-852.

(28) Nair, A. C.; Jayatilleke, P.; Wang, X.; Miertus, S.; Welsh, W. J. Computational studies on tetrahydropyrimidine-2-one HIV-1 protease inhibitors: improving three-dimensional quantitative structure-activity relationship comparative molecular field analysis models by inclusion of calculated inhibitor- and receptor-based properties. *Journal of Medicinal Chemistry* **2002**, *45*, 973-983.

(29) Pungpo, P.; Hannongbua, S. Three-dimensional quantitative structure-activity relationships study on HIV-1 reverse transcriptase inhibitors in the class of dipyridodiazepinone derivatives, using comparative molecular field analysis. *Journal of Molecular Graphics & Modelling* **2000**, *18*, 581-590.

(30) Jayatilleke, P. R. N.; Nair, A. C.; Zauhar, R.; Welsh, W. J. Computational Studies on HIV-1 Protease Inhibitors: Influence of Calculated Inhibitor-Enzyme Binding Affinities on the Statistical Quality of 3D-QSAR CoMFA Models. *Journal of Medicinal Chemistry* **2000**, *43*, 4446-4451.

(31) Barreca, M. L.; Carotti, A.; Carrieri, A.; Chimirri, A.; Monforte, A. M. et al. Comparative molecular field analysis (CoMFA) and docking studies of non-nucleoside HIV-1 RT inhibitors (NNIs). *Bioorganic & Medicinal Chemistry* **1999**, *7*, 2283-2292.

(32) Hilgeroth, A.; Fleischer, R.; Wiese, M.; Heinemann, F. W. Comparison of azacyclic urea A-98881 as HIV-1 protease inhibitor with cage dimeric N-benzyl 4-(4-methoxyphenyl)-1,4-dihydropyridine as representative of a novel class of HIV-1 protease inhibitors: a molecular modeling study. *Journal of Computer-Aided Molecular Design* **1999**, *13*, 233-242.

(33) Debnath, A. K. Three-Dimensional Quantitative Structure-Activity Relationship Study on Cyclic Urea Derivatives as HIV-1 Protease Inhibitors: Application of Comparative Molecular Field Analysis. *Journal of Medicinal Chemistry* **1999**, *42*, 249-259.

(34) Raghavan, K.; Buolamwini, J. K.; Fesen, M. R.; Pommier, Y.; Kohn, K. W. et al. Three-Dimensional Quantitative Structure-Activity Relationship (QSAR) of HIV

Integrase Inhibitors: A Comparative Molecular Field Analysis (CoMFA) Study. *Journal of Medicinal Chemistry* **1995**, *38*, 890-897.

(35) Oprea, T. I.; Waller, C. L.; Marshall, G. R. 3D-QSAR of human immunodeficiency virus (I) protease inhibitors. III. Interpretation of CoMFA results. *Drug Design and Discovery* **1994**, *12*, 29-51.

(36) Debnath, A. K.; Jiang, S.; Strick, N.; Lin, K.; Haberfield, P. et al. Three-Dimensional Structure-Activity Analysis of a Series of Porphyrin Derivatives with Anti-HIV-1 Activity Targeted to the V3 Loop of the gp120 Envelope Glycoprotein of the Human Immunodeficiency Virus Type 1. *Journal of Medicinal Chemistry* **1994**, *37*, 1099-1108.

(37) Zhou, Z.; Madrid, M.; Madura, J. D. New Non-nucleoside Inhibitors in HIV-1 RT Docking Calculations. *Proteins: Structure, Function Genetics* **2002**, *49*, 529-542.

(38) Hannongbua, S.; Pungpo, P.; Limtrakul, J.; Wolschann, P. Quantitative structure-activity relationships and comparative molecular field analysis of TIBO derivatised HIV-1 reverse transcriptase inhibitors. *Journal of Computer-Aided Molecular Design* **1999**, *13*, 563-577.

(39) Huuskonen, J. QSAR Modeling with the Electrotopological State: TIBO Derivatives. *J. Chem. Inf. Comput. Sci.* **2001**, *41*, 425-429.

(40) Garg, R.; Gupta, S. P.; Gao, H.; Babu, M. S.; Debnath, A. K. et al. Comparative Quantitative Structure-Activity Relationship Studies on Anti-HIV Drugs. *Chem. Rev.* **1999**, *99*, 3525-3602.

(41) Smith, M. B. K.; Lamb, M. L.; Tirado-Rives, J.; Jorgensen, W. L.; Michejda, C. J. et al. Monte Carlo calculations on HIV-1 reverse transcriptase complexed with the

non-nucleoside inhibitor 8-Cl TIBO: contribution of the L100I and Y181C variants to protein stability and biological activity. *Protein Engineering* **2000**, *13*, 413-421.

(42) Smith, R. H., Jr.; Jorgensen, W. L.; Tirado-Rives, J.; Lamb, M. L.; Janssen, P. A. J. et al. Prediction of Binding Affinities for TIBO Inhibitors of HIV-1 Reverse Transcriptase Using Monte Carlo Simulations in a Linear Response Method. *Journal of Medicinal Chemistry* **1998**, *41*, 5272-5286.

(43) Cui, M.; Huang, X.; Luo, X.; Briggs, J. M.; Ji, R. et al. Molecular Docking and 3D-QSAR Studies on Gag Peptide Analogue Inhibitors Interacting with Human Cyclophilin A. *Journal of Medicinal Chemistry* **2002**, *45*, 5249-5259.

(44) Buolamwini, J. K.; Assefa, H. CoMFA and CoMSIA 3D QSAR and Docking Studies on Conformationally-Restrained Cinnamoyl HIV-1 Integrase Inhibitors: Exploration of a Binding Mode at the Active Site. *J. of Medicinal Chemistry* **2002**, *45*, 841-852.

(45) Muegge, I.; Podlogar, B. L. 3D-quantitative structure activity relationships of biphenyl carboxylic acid MMP-3 inhibitors: exploring automated docking as alignment method. *Quantitative Structure-Activity Relationships* **2001**, *20*, 215-222.

(46) Jones, G.; Willett, P.; Glen, R. C.; Leach, A. R.; Taylor, R. Development and validation of a genetic algorithm for flexible docking. *Journal of Molecular Biology* **1997**, *267*, 727-748.

(47) Weiner, S. J.; Kollman, P. A.; Case, D. A.; Singh, U. C.; Ghio, C. et al. A New Force Field for Molecular Mechanical Simulation of Nucleic Acids and Proteins. *J. Am. Chem. Soc.* **1984**, *106*, 765.

(48) Gasteiger, J.; Marsili, M. Iterative Partial Equalization of Orbital Electronegativity - A Rapid Access to Atomic Charges. *Tetrahedron* **1980**, *36*, 3219.

(49) Kukla, M. J.; Breslin, H. J.; Pauwels, R.; Fedde, C. L.; Miranda, M. et al. Synthesis and anti-HIV-1 activity of 4,5,6,7-tetrahydro-5-methylimidazo[4,5,1-jk][1,4]benzodiazepin-2(1H)-one (TIBO) derivatives. *Journal of Medicinal Chemistry* **1991**, *34*, 746-751.

(50) Kukla, M. J.; Breslin, H. J.; Diamond, C. J.; Grous, P. P.; Ho, C. Y. et al. Synthesis and anti-HIV-1 activity of 4,5,6,7-tetrahydro-5-methylimidazo[4,5,1-jk][1,4]benzodiazepin-2(1H)-one (TIBO) derivatives. 2. *Journal of Medicinal Chemistry* **1991**, *34*, 3187-3197.

(51) Breslin, H. J.; Kukla, M. J.; Ludovici, D. W.; Mohrbacher, R.; Ho, W. et al. Synthesis and Anti-HIV-1 Activity of 4,5,6,7-Tetrahydro-5-methylimidazo[4,5,1-jk][1,4]benzodiazepin-2(1H)-one (TIBO) Derivatives. 3. *Journal of Medicinal Chemistry* **1995**, *38*, 771-793.

(52) Ho, W.; Kukla, M. J.; Breslin, H. J.; Ludovici, D. W.; Grous, P. P. et al. Synthesis and Anti-HIV-1 Activity of 4,5,6,7-Tetrahydro-5-methylimidazo[4,5,1-jk][1,4]benzodiazepin-2(1H)-one (TlBO) Derivatives. 4. *Journal of Medicinal Chemistry* **1995**, *38*, 794-802.

(53) Breslin, H. J.; Kukla, M. J.; Kromis, T.; Cullis, H.; De Knaep, F. et al. Synthesis and anti-HIV activity of 1,3,4,5-tetrahydro-2H-1,4-benzodiazepin-2-one (TBO) derivatives. Truncated 4,5,6,7-tetrahydro-5-methylimidazo[4,5,1-jk][1,4]benzodiazepin-2(1,H)-ones (TIBO) analogues. *Bioorganic & Medicinal Chemistry* **1999**, *7*, 2427-2436.

(54) Solis, F. J.; EWets, R. J.-B. Minimization by randon search techniques. *Mathematical Operations Research* **1981**, *6*, 19-30.

(55) L'Ecuyer, P.; Cote, S. Implementing a redom number package with splitting facilities. *ACM Transactions on Mathematical Software* **1991**, *17*, 98-111.

Table 1. Structures and HIV-1 RT Inhibitory Activity of Compounds used in the Work.

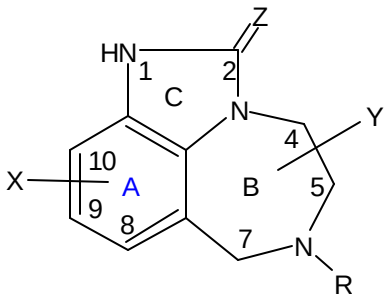

Compd.	X	Z	R	Y	pIC_{50}
1	H	S	DMA[a]	5-Me(S)	7.36
2	9-Cl	S	DMA	5-Me(S)	7.47
3	8-Cl	S	DMA	5-Me(S)	8.37
4	8-F	S	DMA	5-Me(S)	8.24
5	8-SMe	S	DMA	5-Me(S)	8.30
6	8-OMe	S	DMA	5-Me(S)	7.47
7	8-OC_2H_5	S	DMA	5-Me(S)	7.02
8	8-CN	S	DMA	5-Me(S)	7.25
9	8-CHO	S	DMA	5-Me(S)	6.73
10	8-$CONH_2$	O	DMA	5-Me(S)	5.20
11	8-Br	O	DMA	5-Me(S)	7.33
12	8-Br	S	DMA	5-Me(S)	8.52
13	8-I	O	DMA	5-Me(S)	7.06
14	8-I	S	DMA	5-Me(S)	7.32

15	8-C=-CH	S	DMA	5-Me(S)	7.53
16	8-Me	O	DMA	5-Me(S)	6.00
17	8-Me	S	DMA	5-Me(S)	7.87
18	8-NH_2	O	CPM[b]	5-Me(S)	3.07
19	8-NMe_2	O	CPM	5-Me(S)	5.18
20	9-NH_2	O	CPM	5-Me(S)	4.22
21	9-NMe_2	O	CPM	5-Me(S)	5.18
22	9-NHCOMe	O	CPM	5-Me(S)	3.80
23	9-NO_2	S	CPM	5-Me(S)	5.61
24	9-F	S	DMA	5-Me(S)	7.60
25	9-CF_3	O	DMA	5-Me(S)	5.23
26	9-CF_3	S	DMA	5-Me(S)	6.31
27	10-OMe	O	DMA	5-Me(S)	5.18
28	10-OMe	S	DMA	5-Me(S)	5.33
29	9,10-di-Cl	S	DMA	5-Me(S)	7.60
30	10-Br	S	DMA	5-Me(S)	5.97
31	H	O	$CH_2CH=CH_2$	5-Me(S)	4.15
32	H	O	2-MA	5-Me(S)	4.33
33	H	O	CH_2CO_2Me	5-Me(S)	3.04
34	H	O	CH_2-2-furanyl	5-Me(S)	3.97
35	H	O	$CH_2CH_2CH=CH_2$	5-Me(S)	4.30
36	H	O	$CH_2CH_2CH_3$	5-Me(S)	4.05
37	H	O	CPM	5-Me(S)	4.36

38	H	O	$CH_2CH=CHMe(E)$	5-Me(S)	4.24
39	H	O	$CH_2CH=CHMe(Z)$	5-Me(S)	4.46
40	H	O	$CH_2CH_2CH_2Me$	5-Me(S)	4.00
41	H	O	DMA	5-Me(S)	4.90
42	H	O	$CH_2C(Br)=CH_2$	5-Me(S)	4.21
43	H	O	$CH_2C(Me)=CHMe(E)$	5-Me(S)	4.54
44	H	O	$CH_2C(C_2H_5)=CH_2$	5-Me(S)	4.43
45	H	O	$CH_2CH=CHC_6H_5(Z)$	5-Me(S)	3.91
46	H	O	$CH_2C(CH=CH_2)=CH_2$	5-Me(S)	4.15
47	8-Cl	S	DMA	H	7.34
48	9-Cl	S	DMA	H	6.80
49	9-Cl	O	DMA	5-Me(S)	6.74
50	9-Cl	S	CPM	5-Me(S)	7.47
51	H	S	CPM	5-Me(S)	7.22
52	H	O	DMA	5-Me(S)	5.48

[a] 3,3-Dimethylallyl. [b] Cyclopropylmethyl. [c] 2-Methylallyl.

Table 2. The Comparison of PLS Statistics Results of 3D QSAR Models of CoMFA and CoMSIA

	Docking alignment		Atom Fit alignment	
	CoMFA	CoMSIA	CoMFA	CoMSIA
PCs	4	5	6	6
r^2	0.962	0.948	0.959	0.916
q^2	0.701	0.708	0.661	0.680
SE_{press}	0.326	0.381	0.335	0.482
		fraction		
steric	0.41	0.077	0.50	0.070
electrostatic	0.59	0.224	0.50	0.246
hydrophobic		0.483		0.453
H-acceptor		0.216		0.231

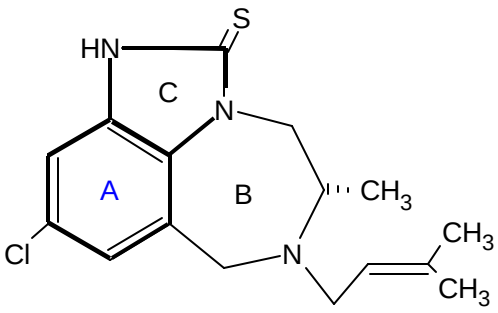

Figure 1. The molecule used as template for molecule alignment. The bold part is the core for alignment.

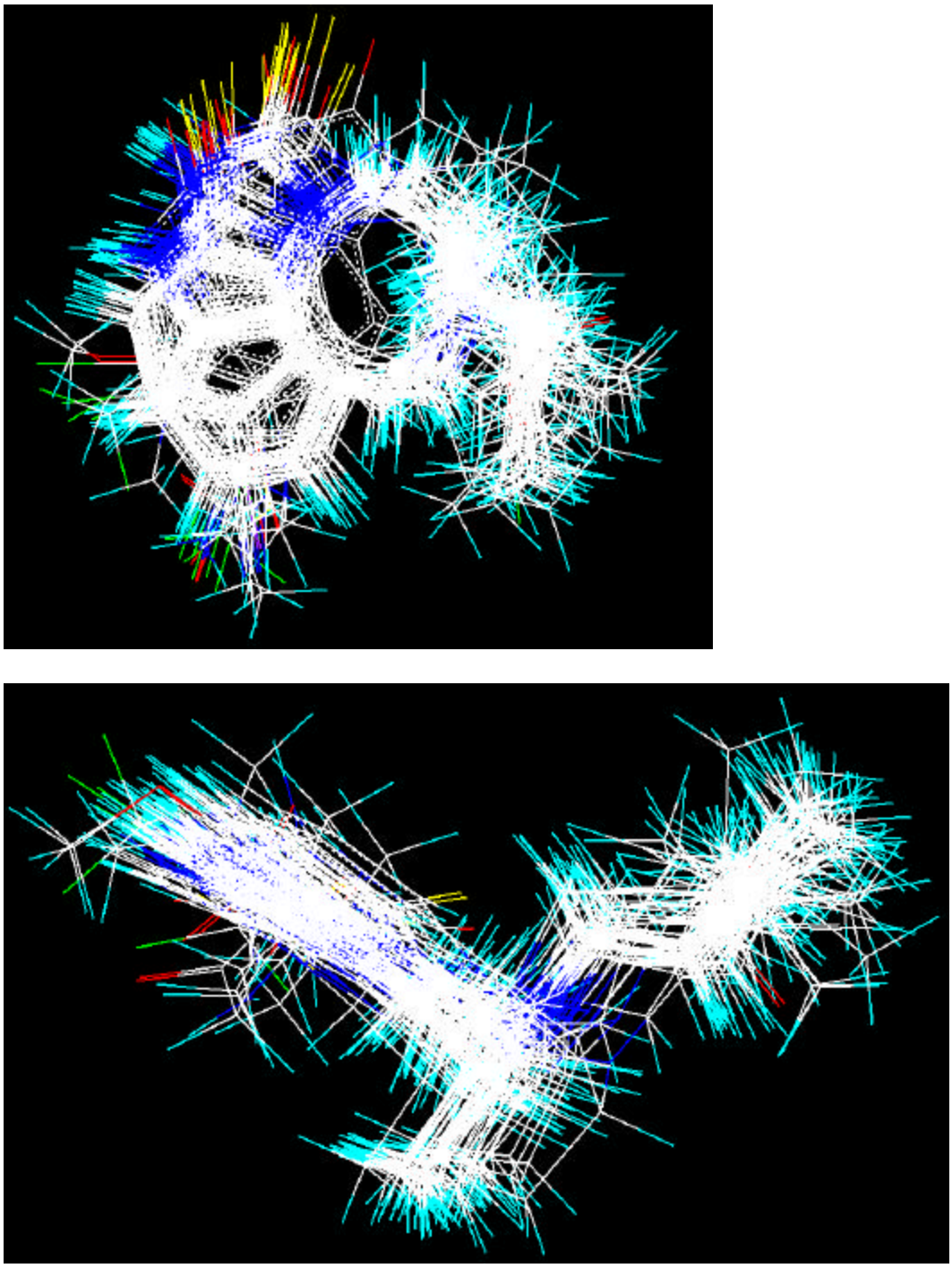

Figure 2. Superposition of all TIBOs aligned by the Autodock.

All molecules are aligned according the bound position in the non-nucleoside binding pocket of RT using flexible docking (Autodock3).

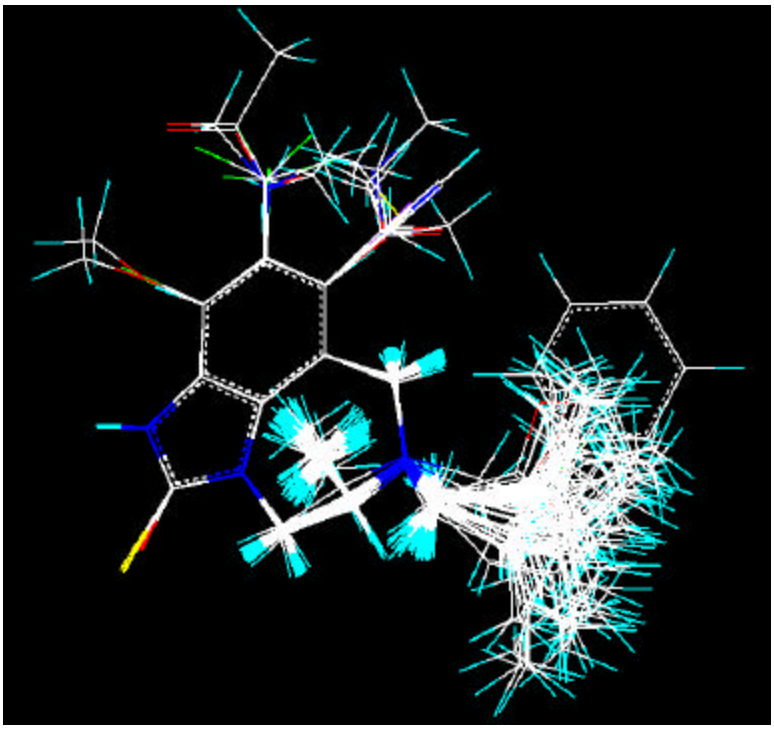

Figure 3. Superposition of all TIBOs aligned by atom fit, in which all molecules are aligned according to core atoms in the ring A and ring C (see **Figure 1** for ring A and ring C).

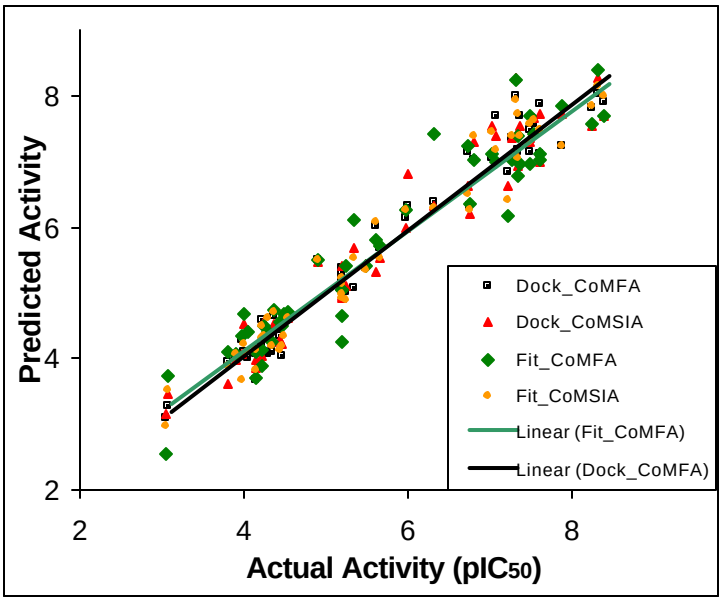

Figure 4. Experimental activity (pIC_{50}) vs. Calculated activity values of 3D QSAR Models.

The black squares and red triangles are CoMFA and CoMSIA results based on docking alignment and conformation determination. The green diamonds and yellow cycles are CoMFA and CoMSIA results based on atom fit alignment and docking conformation determination. The black line is the trend line of the CoMFA model of docking and the green line is the trend line of the CoMFA model of atom fit. The two set data nearly have same trend lines.

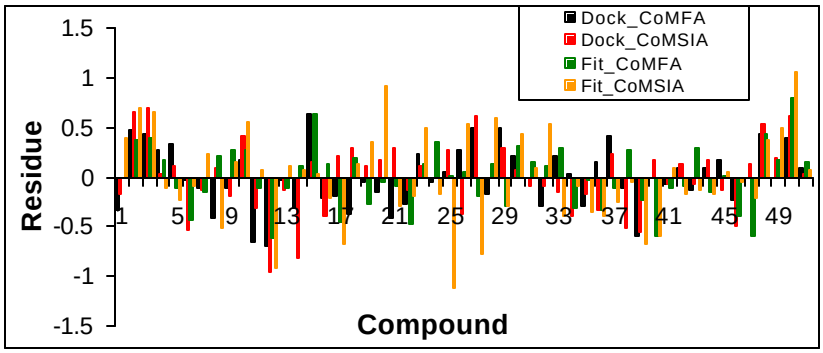

Figure 5. The residuals between experimental activities and predicted activities from the four QSAR models.

The black and red bars are CoMFA and CoMSIA results based on docking alignment and conformation determination. The green and yellow bars are CoMFA and CoMSIA results based on atom fit alignment and docking conformation determination.

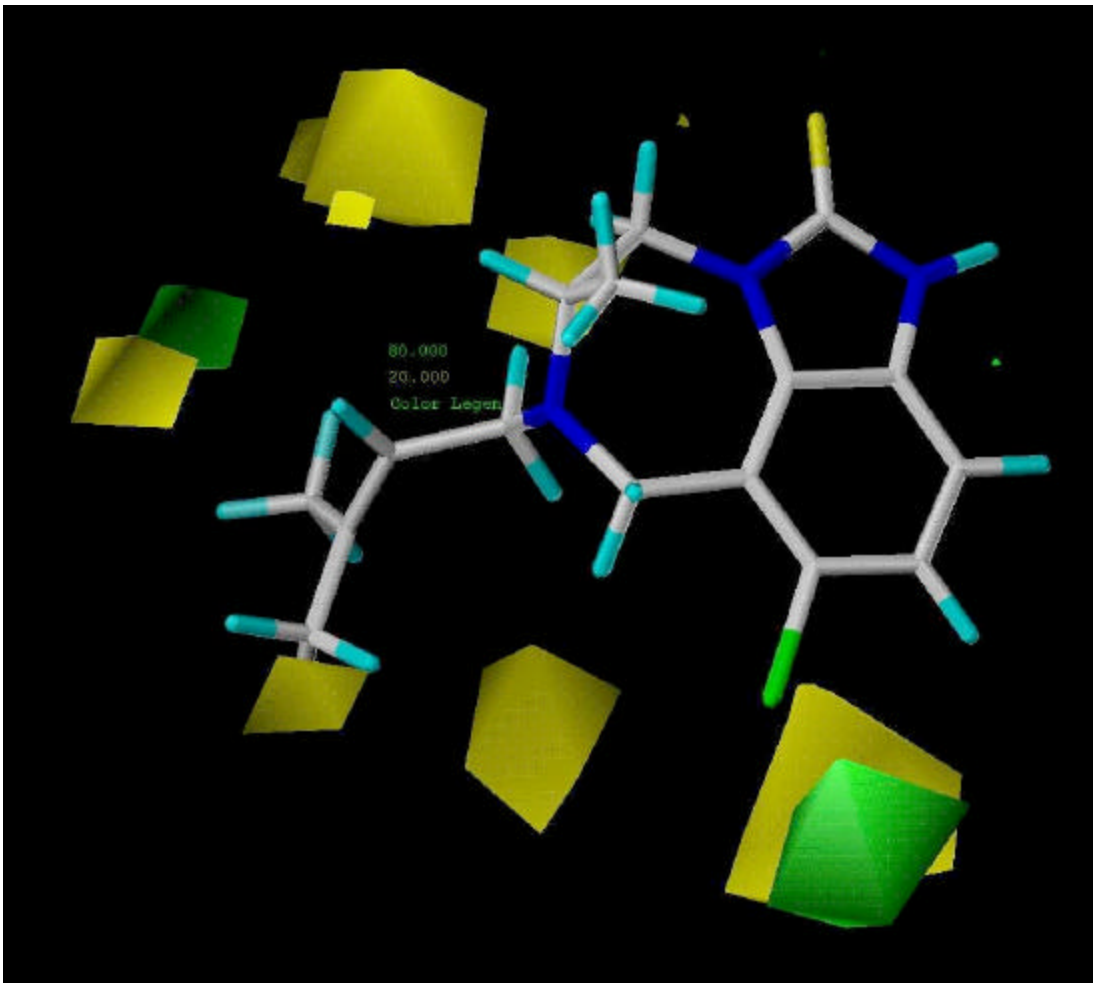

Figure 6. Steric contour maps of the CoMFA model from the docking alignment.

8-Cl-TIBO (Tivirapine, pIC_{50} =8.37) is used to demonstrate the corresponding areas where a change on molecule may affect its activity. Green contours indicate the regions where the addition of bulky groups may increase activity. Yellow contours indicate the regions where the addition of bulky groups may decrease activity.

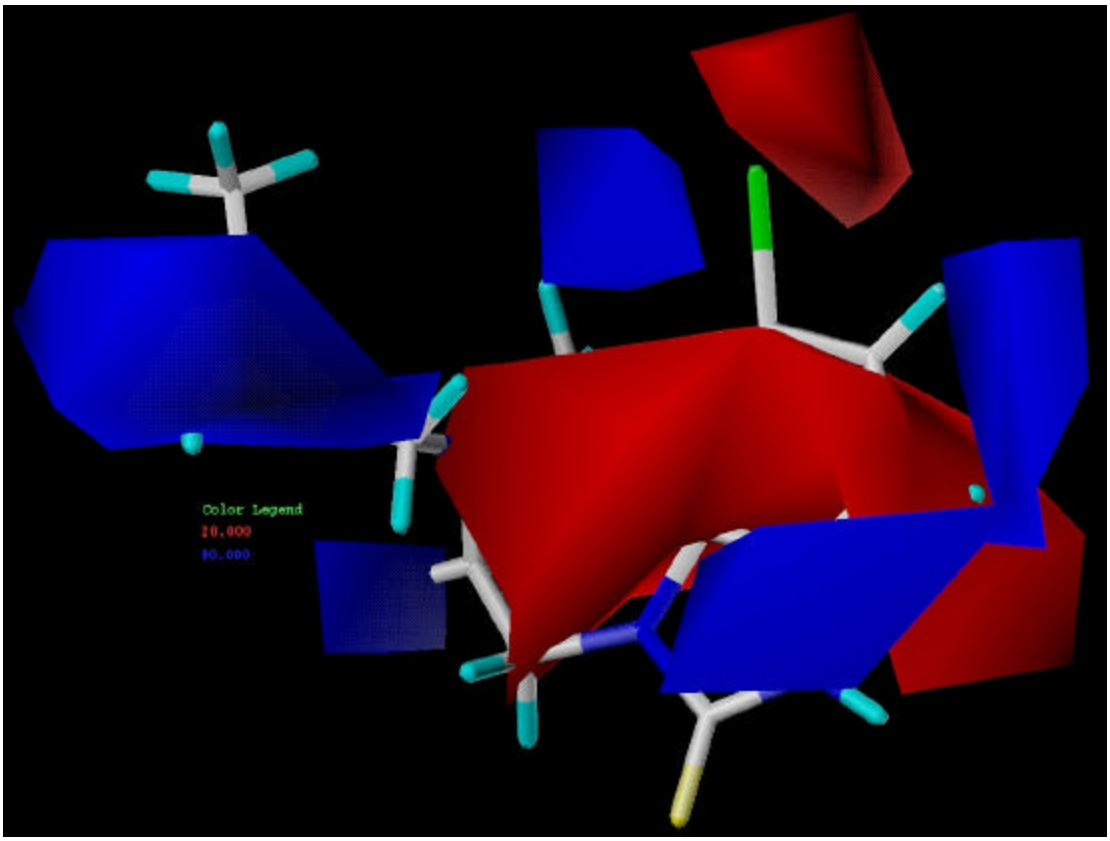

Figure 7. Electrostatic contour of the CoMFA model from docking alignment.

8-Cl-TIBO (Tivirapine, pIC_{50} =8.37) is used to demonstrate the corresponding areas where a change on molecule may affect its activity. Blue contours indicate regions where positive groups may increase activity. Red contours indicate regions where negative groups may increase activity.

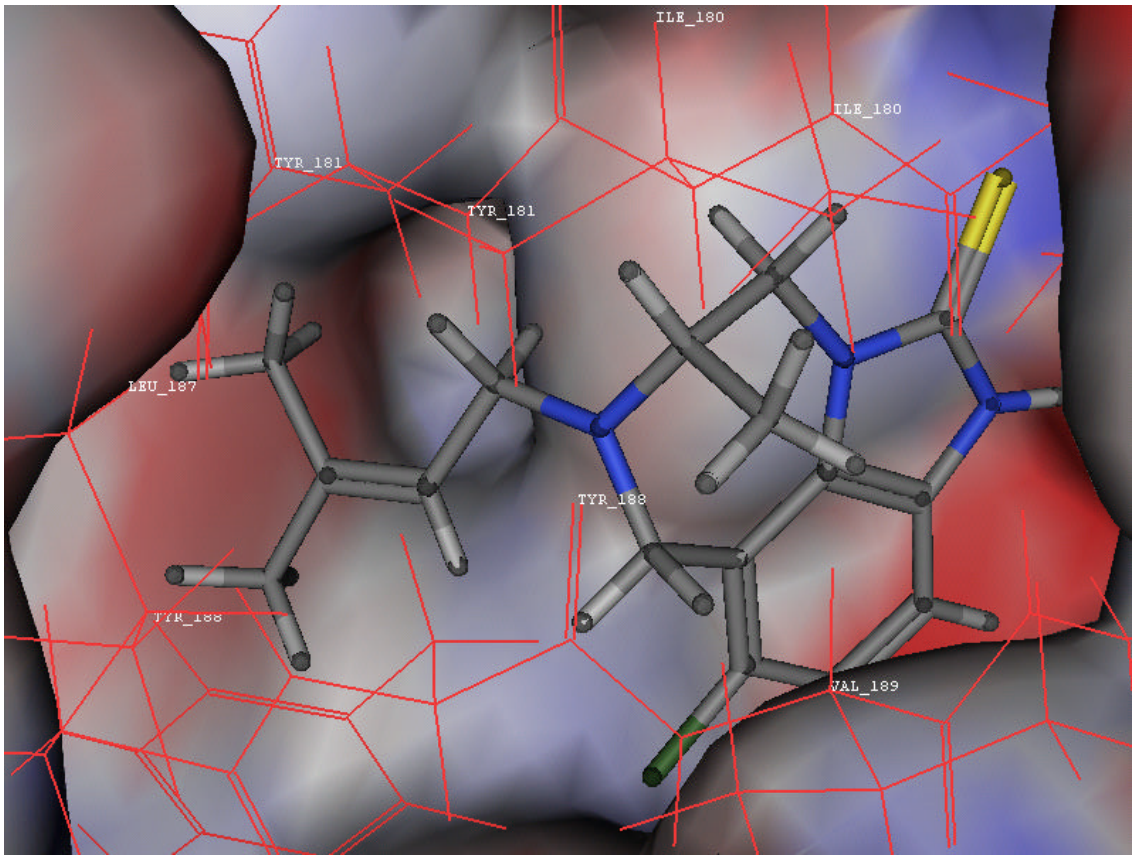

Figure 8. The actual binding structure of compound 3 (superposed on compound 2) from crystal structure. The blue is positive area and red is negative area calculated from RT.

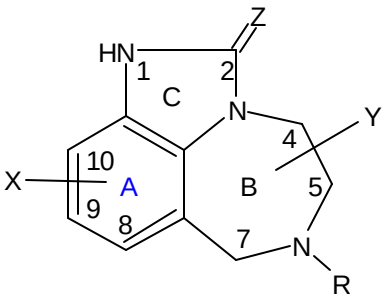

Structure in **Table 1**

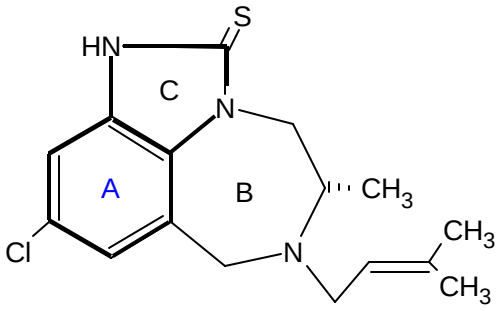

Structure in **Figure 1**.